FFI Norwegian Defence Research Establishment

21/00895

FFI-RAPPORT

Array antennas with defunct elements, a computational study

Kyrre Strøm

Array antennas with defunct elements, a computational study

Kyrre Strøm

Norwegian Defence Research Establishment (FFI) 16 June 2021

Keywords
Radar
Signalbehandling
Simulering

FFI report
21/00895

Project number
1440

Electronic ISBN
978-82-464-3358-5

Approvers
Børge Torvik, *Research Manager*
Trygve Sparr, *Research Director*

The document is electronically approved and therefore has no handwritten signature.

Summary

Simulations of transmit and receive properties for a Uniform Linear Array (ULA) antenna with defunct elements have been conducted. Maximum directivity for ULA without tapering is determined by the number of operating elements in the array, independent on the location of the defunct elements, and therefore not altered much by say 10% degradation. The side lobe level for a conventional beamformer with strong side lobe level tapering will, however, on average suffer substantially from degradation. The degradation effect on received SINR for an ULA exposed to a barrage jammer is also studied. Whereas the conventional beamformer is blinded, the minimum variance destortionless response (MVDR) beamformer behaves well and manages to suppress side lobe jamming also in the case of 10% defunct elements. The same result holds for ULA with fully overlapping subarrays and the beam space minimum variance beamformer, as long as the jammer is located within the fan-sector of the overlapping subarrays beam fan.

Sammendrag

Simuleringer av egenskaper ved sending og mottak til en Uniform Linear Array (ULA) antenne med ikke-fungerende antenneelementer er utført. Maksimum direktivitet for ULA uten sidelobedemping er bestemt av antall oprative elementer i arrayen, uavhengig av plasseringen til de ikke-fungerende elementene, og derfor ikke endret mye ved si 10% degradering. Imidlertid vil sidelobenivået til en konvensjonell beamformer med sterk sidelobedempning lide betydelig ved degradering. Effekten av degradering på oppnådd SINR for en ULA utsatt for en støyjammer er også studert. Mens den konvensjonelle beamformeren blir blendet, oppfører minimum varians forvrengningsfri respons (MVDR) beamformeren seg bra, og klarer å undertrykke sidelobejamming også når 10% av elementene er ikke-fungerende. Det samme holder for ULA med fullt overlappende sub-arrayer og beamspace minimum varians beamformeren sålenge jammeren befinner seg innen vifte-sektoren til stråleviften for de overlappende sub-arrayene.

Contents

1 Introduction

An array antenna consists of many Transmit Receive Module (TRM)s. Some of them may break down without deteriorating the antenna performance too much. The phrase "'graceful degradation"' is sometimes used for describing this property. Robustness against degradation is important and would typically be considered during the process of contracting new Active electronically scanned array (AESA) or Passive electronically scanned array (PESA) radars.

This note is a computational study on the impact of impaired elements on properties like array gain and directivity. We will only consider impaired elements that are fully defunct. Most of the simulations treat a 10% degraded Uniform Linear Array (ULA) of 30 elements and its performance for the ensemble of all possible realisations with three defunct elements, or for a large subset of these realisations. Mean performance values over the realisations are shown as functions of input parameters like signal strength and angular distance between jammer and target. The ability to mitigate a barrage jammer is studied for the Minimum Variance Distortionless Response (MVDR) beamformer with various degrees of diagonal loading. Also, the MVDR beamspace method for overlapping subarrays is studied. Adaptive beamforming is computationally demanding and real time processing may require the reduction in Degrees of Freedom (DoF) that can be offered by beamspace methods [3]. Moreover, large array antennas usually group their elements into subarrays before digitalization and thereby reduce the received amount of data to a managable volume. Even for antennas with a controllable decay in performance with increasing number of defunct TRMs, there is a maximum tolerable number before the antenna stops operating meaningfully. We start out in the next section by considering a statistical model relating the likely operational status of a single TRM to the operational status of the whole array antenna. Textbooks on array processing are given by [4], [2].

2 System availability

A monopulse system with three receiver channels for the sum and delta beams will stop operating when one of the channels break down. An array radar with several TRMs may, however, continue operating after breakdown of one or more of the TRMs. The array system might fulfill necessary quality measures as long as no more than a given percentage of the TRMs are defunct. We follow the discussion in [1] and use the phrase availability to denote the probability that an object is functioning satisfactorily at a given time. In this context availability will be used about a single TRM and about the whole array antenna system. We assume that a TRM is either functioning well or is totally defunct. If the availability of a single TRM is a, the probability that exactly k out of the N TRMs are available follows the binomial distribution. This is the kth Bernstein polynomial in a of degree N, $\binom{N}{k}a^k(1-a)^{N-k}$. Assuming the array system can tolerate as much as M defunct elements, the system availability is

$$P_{sys,M}(a) = \sum_{k=N-M}^{N} \binom{N}{k} a^k (1-a)^{N-k}$$

In Figure 2.1 we have plotted the system availability as function of a single element availability for an array antenna of 30 elements that can tolerate maximum M defunct elements, $M = 0, 1, \ldots, 6$ where $M = 6$ is 20% of the elements. We assume there is one TRM for each element. The availability for a monopulse system with three receiver channels is also depicted. When looking at the figure one should have in mind the probability of failure for a monopulse channel in general will be different from the probability of failure for an antenna element in a large array antenna.

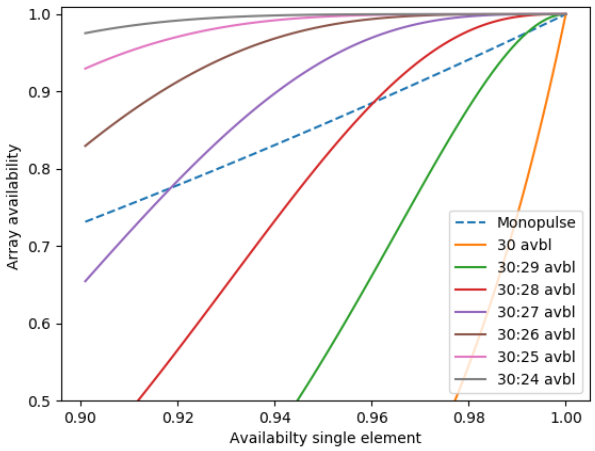

Figure 2.1 System availability as function of single channel availability for monopulse radar, and for array antenna of 30 elements that can tolerate M defunct elements, $M = 0, \ldots, 6$.

As an example assume the availability for each of the TRMs is 0.96. Then the green curve in Figure 2.1 indicates the probability is less than 70% that the ULA-30 will be operational if it can

tolerate maximum 1 defunct TRM. Whereas the violet curve indicates the availability is more than 0.95 for the ULA-30 that can tolerate as much as three defunct TRMs.

3 Directivity

The directivity in a direction for an antenna is the radiant intensity in the direction divided by the average radiant intensity over all directions. Radiant intensity is the power transmitted (or received) per unit solid angle. Antenna directivity is often used synonymous with maximum directivity. We will, however, us the phrase *directivity* for any specified direction. For an array antenna of N elements with steering vector $s(\eta)$ in direction η and beamformer $w \in \mathbb{C}^N$, the directivity in direction η is

$$D(\eta) = 4\pi \frac{|w^h s(\eta)|^2}{\int_{\mathbb{S}_2} w^h s(\xi) s^h(\xi) w d\xi} = \frac{|w^h s(\eta)|^2}{w^h B w}$$

where the matrix B has components

$$B_{ij} = \frac{1}{4\pi} \int_{\mathbb{S}_2} s_i(\xi) s_j^*(\xi) d\xi$$

A beamformer is a spatial linear filter that scales, phase shifts and sums the signal outputs from each of the N receiver channels of an array antenna. It is represented by a complex N-vector $w \in \mathbb{C}^N$. For an array antenna with isotropic unit gain elements, the steering vector is the array response to a planar monochromatic wave of unite amplitude from direction η. For a ULA of N isotropic elements and element spacing d, the steering vector s has components

$$s_k = \exp\left(i2\pi \frac{d}{\lambda} k \sin(\vartheta)\right), \quad k = (1-N)/2, \ldots, (N-1)/2$$

Here ϑ is the angle between the array axis normal plane and the signal direction of arrival. Taking the array axis as the first coordinate axis, and letting φ be the rotation angle around the array axis, the 3-space direction vector η can be expressed in terms of ϑ as $\eta = (\sin\vartheta, \cos\vartheta\cos\varphi, \cos\vartheta\sin\varphi)$. In the ULA case the average intensity matrix has components given by simple expression of the sinc function

$$B_{jk} = \operatorname{sinc}\left(2\pi \frac{d}{\lambda}(j-k)\right)$$

Here $\operatorname{sinc}(x) = \sin(x)/x$. These components are independent on the number of elements in the array, only the distance d between the elements matter. In our Matlab simulations of degraded antennas we assume the impaired elements are turned off, resulting in steering vectors with zero value components for the impaired elements. Similarly the power matrix components corresponding to at least one impaired element is set to zero. Alternatively, we obtain the same result by nulling the beamformer weight corresponding to the defunct elements when calculating beamformer response average directivity. The uniform beamformer has weights given by the steering vector scanned to the desired direction. In this case the beamformer response $w^h s(\eta) = \sum_{k, w_k \neq 0} |s_k(\eta)|^2 = N - L$ where L is the number of defunct elements. The maximum beamformer response is the same no matter which of the elements are turned off. When the element spacing is half the wavelength, the matrix $B = I$ is the identity matrix and the average intensity for any beamformer is $w^h B w = |w|_2^2$. For the uniform beamformer all weights have unit magnitude, and setting L of them to zero results in $|w|_2^2 = N - L$. Thus

$$\max D(\eta) = N - L \text{ when } \frac{d}{\lambda} = 0.5 \text{ uniform weights and } N - L \text{ operating elements}$$

For other inter element spacings or for non-uniform weights the max directivity will vary somewhat depending on the ordering of the L defunct elements within the N array elements. In other directions than the desired scan direction, the variation among the L-degradations of the N array is greater. We will use the phrase **L-degradation** to denote *an array with exactly L defunct elements and where the defunct elements make a specific subset of all the array elements*. For an array of N elements there are $\binom{N}{L}$ possible L-degradations. The directivity for a ULA-30 using the conventional beamformer without tapering, and the directivities for all the 30 possible choices of 1-degradations are calculated by Matlab scripts and depicted in Figure 3.1. The element spacing to wavelength ratio is $d/\lambda = 0.5$, and this ratio will be adopted in all the plots of these notes unless otherwise stated. Beam pointing direction is 20° from boresight for the plots of this section.

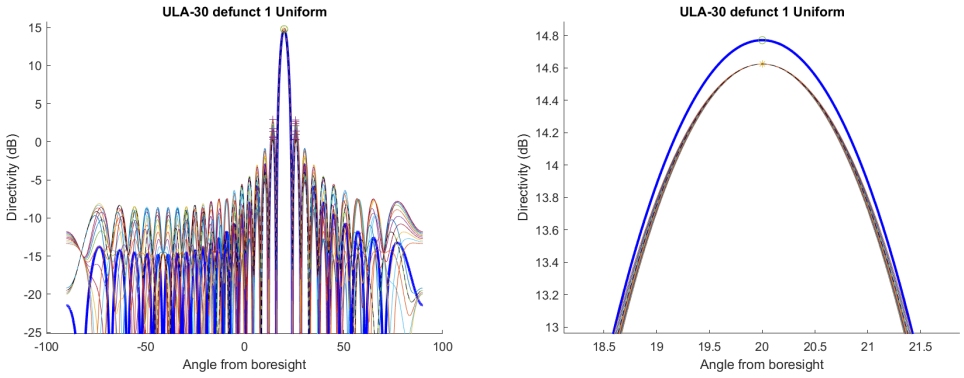

Figure 3.1 Directivity of ULA-30 uniform beam (fat blue) and all 1-degradations, left panel. Right panel zooms in on directivity in pointing direction at 20° *from boresight.*

Directivies for ULA-30 with Dolph-Chebyshev -30dB Side lobe level (SLL) tapering and all possible 1-degradations are depicted in Figure 3.2. The Dolph-Chebyshev taper for the full array is used also for the 1-degradations, giving the same results as nulling the weight corresponding to defunct element.

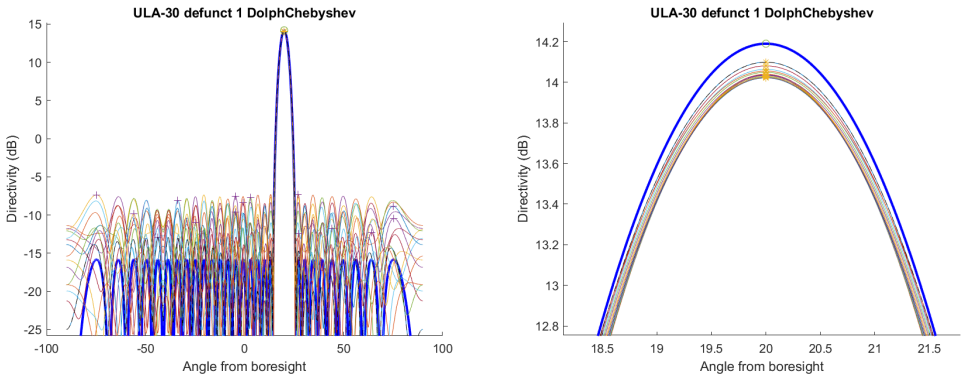

Figure 3.2 Directivity of ULA-30 Dolph-Chebyshev taper (fat blue) and all 1-degradations, left panel. Right panel zoom on directivity in pointing direction.

There are small variations in max Directivity, less than 1 dB for the Dolph-Chebyshev taper and no

variation at all for the uniform beamformer among the 1-degradations. In general, the SLL increases when one or more elements are defunct, in particular for the Dolph-Chebyshev tapered beamformer. However, the maximum SLL for the uniform beamformer varies with the degradations on both sides of the -13dB level for the non-degraded array. Figure 3.3 shows the distribution of maximum SLL relative to main lobe level among all the 4060 possible 3-degradations for the ULA-30 array with uniform tapering. Left panel shows distribution for the uniform beamformer and the right panel using the taper for the Dolph-Chebyshev -30dB SLL.

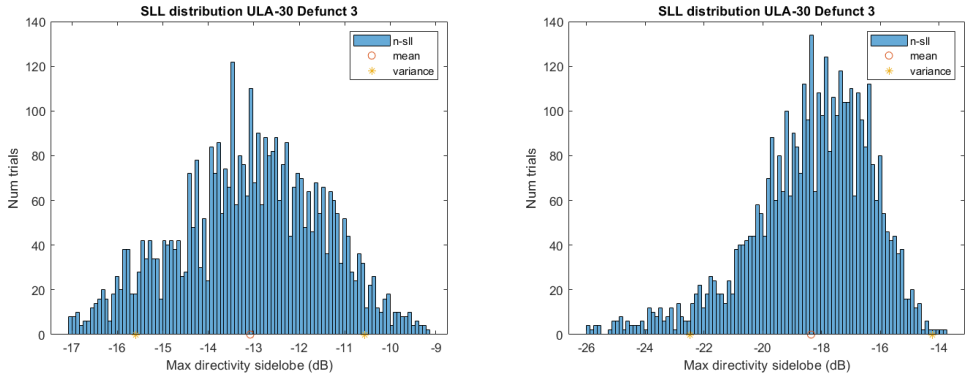

Figure 3.3 Distribution of max SLL directivity relative to mainlobe peak for all 3-degradations of ULA-30 steered to 20° from boresight. Left panel depicts non-tapering, and right panel Dolph-Chebyshev tapering.

In the right panel of Figure 3.3 we see that the low SLL is more or less completely destroyed for the Dolph-Chebyshev taper except for a few 3-degradations that keep the SLL reasonably well. In transmit mode one usually wants the full transmit power from all the antenna elements, and strong SLL tapering would not be applied unless there are special reasons for not illuminating areas outside the main lobe. For the uniform beamformer of a non-degraded array antenna the maximum SLL relative to the main lobe is approximately -13dB, even when steered to 20° as is the case here. The max SLL for the 3-degradations of the ULA-30 shown in Figure 3.3 vary on both sides of this value. The minimum value of -17dB is taken for the two 3-degradations with defunct elements number [3, 6, 26] and [5, 25, 28], depicted in Figure 3.4. The directivity patterns are identical for the two. Thus in these two special cases there is a notable improvement in max SLL, a substantial reduction of 4dB in peak SLL is obtained simply by turning off three elements. We note, however, that the SLL farther apart from the main lobe is increased relative the non-dedegraded uniform beam.

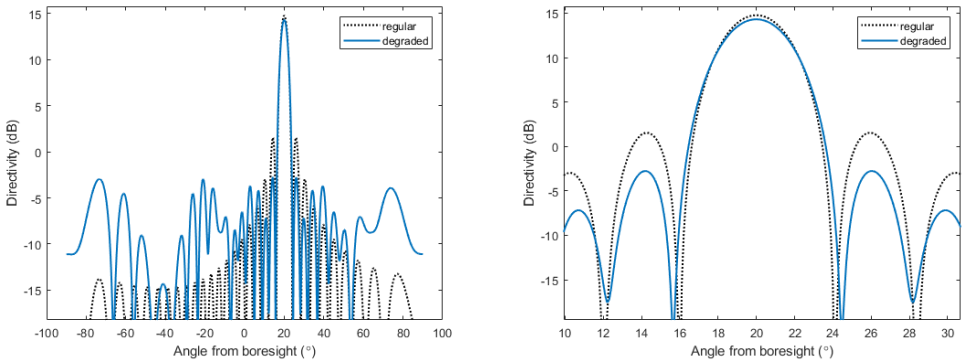

Figure 3.4 Directivity uniform beamformer for the ULA-30 with the 3-degradation of lowest SLL. Right panel zooms in on mainlobe.

High SLLs is unfortunate in recieve mode, since multipath reflections and jammer interference in the side lobes may hide the target signal completely. So far we only considered the conventional beamformer with no taper or with Dolph-Chebyshev taper. In the next section we shall see the adaptive beamformers provide higher array gain in receive mode than the conventional one when the array is exposed to interference.

4 Array receiver gain

In this section we look at how the array gain on receive is affected by antenna degradation. Like in Chapter 3 we assume any impaired element is totally shut off. We start by making some assumptions about the received signal. A snapshot x of the output from the antenna element array consists of noise, interference from a barrage jammer and target signal, $x = x_{ni} + s$ where x_{ni} is the thermal noise plus interference part. Moreover, we will assume the target signal s is independent from x_{ni}. The spatial filter made by a beamformer $w \in \mathbb{C}^N$ has signal power response $|w^h s|^2$, and noise power response $\varepsilon\left(|w^h x_{ni}|^2\right) = w^h K w$. In practice extracting the target signal from the full signal is challenging and an estimate for the signal power is $\varepsilon(\left(w^h x x^h w\right) = w^h R w$. Here K is the noise plus interference spatial covariance matrix and R is the full signal spatial correlation matrix,

$$K = \varepsilon(x_{ni} x_{ni}^h), \quad R = \varepsilon(x x^h) = K + s s^h$$

In our simulations we will estimate the Signal to Interference plus Noise Ratio (SINR) to be

$$\text{SINR} = \frac{w^h R w}{w^h K w} = 1 + \frac{|w^h s|^2}{w^h K w}$$

where the latter equality holds since the target signal is assumed statistically independent from the noise plus interference.

By array gain we understand the ratio between the output SINR from the array beamformer and the SINR output from any of the elements. We assume the element gain is constant and identical for all array elements, and the elements have independent thermal noise at the same intensity level. Let SNRe denote the signal to thermal noise ratio output from the TRM of each element. In addition to thermal noise there will be an interfering signal from a barrage jammer. The ratio between jamming signal power and thermal noise output from the TRM of each element is denoted JNRe. The element wise signal to interference pluss noise ratio is SNRe/(1 + JNRe), where SNRe is the element wise signal to thermal noise ratio. Here we have assumed independence of jammer signal from thermal noise. The array gain is then obtained as

$$\text{Array gain} = \text{SINR}\frac{1 + \text{JNRe}}{\text{SNRe}}$$

The factor (1 + JNRe)/SNRe will be constant in our simulation during comparison of a degraded antenna with a non-degraded array, and during comparison of various beamformers. Attention is therefore paid to the SINR output from various array beamformers and array degradations, and the element-wise SINRe will be discarded in most cases when presenting simulation results.

Simulations are run for two types of beamformers. The adaptive MVDR beamformer w_{mv} is given as

$$w_{mv} = \frac{K^{-1} g}{g^h K^{-1} g} \quad \text{where } g = t \odot s \tag{4.1}$$

Here g is the tapered steering vector with tapers t and steering vector $s = s(\eta)$ in the desired direction η. K is the noise plus interference spatial covariance matrix for the array. w_{mv} is the solution to the quadratic problem [2]

$$\min_w w^h K w \quad \text{subject to } w^h g = 1 \tag{4.2}$$

When g is the steering vector in direction η, the solution w_{mv} minimizes the power response to signals from other directions than the desired direction η.

The other type of beamformer considered is the conventional beamformer with tapering t. This is obtained by replacing the covariance matrix K in (4.1) by the identity matrix, giving

$$w_c = g/|g|_2^2 \tag{4.3}$$

Choosing tapers $t = [1, 1, \ldots, 1]^t$ we retrieve the conventional uniform beamformer.

When calculating adaptive beamformers for a given L-degraded antenna, we assume knowledge about which TRMs are defunct. Let J_0 be the set of $N - L$ indices picking all the fully operational array elements for the L-degradation. If x is the output snapshot from the array antenna and w a beamformer for the array, we let $x_0 = x(J_0)$ and $w_0 = w(J_0)$. The beamformer response to the array snapshot is $w^h x = w_0^h x_0$. The submatrix K_0 of non-zero elements in the covariance matrix K has element

$$K_0(i, j) = K(J_0(i), J_0(j))$$

We may write the noise plus interference power response after beamforming as $w^h K w = \varepsilon(w^h x x^h w) = \varepsilon(w_0^h x_0 x_0^h w_0) = w_0^h K_0 w_0$. The correlation matrix R_0 is defined similarly. Assuming some thermal noise, the L-degraded covariance matrix K_0 has full rank. Finally the tapered steering for the L-degraded system is obtained from the original by discarding the defunct elements, $g_0 = g(J_0)$. The quadratic optimization problem defining the MVDR beamformer (4.2) can now be written

$$\min_{w_0} w_0^h K_0 w_0 \quad \text{subject to} \quad w_0^h g_0 = 1 \tag{4.4}$$

and has solution

$$w_{0mv} = \frac{K_0^{-1} g_0}{g_0^h K_0^{-1} g_0}$$

This can be viewed as the MVDR beamformer for a linear array of $N - L$ elements with non-uniform spacing between the elements.

4.1 Simulations ULA all elements digitized

In the MATLAB simulations the barrage jammer is located at 10° from boresight. The jammer power is set to give an elementwise Interference to Noise Ratio (INR) JNRe = $40dB$. In this section and the remainder of this report whenever the simulations are conducted with Dolph-Chebyshev tapered beamformers, the tapering will have SLL -40dB, as opposed to -30dB in the previous section. In the first simulation example the target signal strength is set to give an elementwise Signal to noise ratio (SNR) equal to SNRe = $0dB$, and the target is located at 16° from boresight. Figure 4.1 shows the SINR as a function of the beam pointing direction for the full array of 30 elements and for one realisation of three defunct elements. Beamscan with conventional Beamforming (BF) and with the adaptive MVDR beamformer is performed, no tapering. Diagonal loading with factor 0.1 relative to the normalized trace of the covariance matrix is applied. See Chapter 4.2 for further details on diagonal loading. The MVDR beamformer peaks when pointing at the target, whereas the conventional beamformer has an overall low SINR. Moreover, the conventional beamformer does not have a maximum in direction of the target, but spikes of fairly high SINR appear in the

neighbourhood. The degraded antenna with the three defunct elements [5,6,25] behaves poorly for the conventional beamformer, but the MVDR beamformer achieves almost as high a SINR as the fully operating antenna. Thus for this signal environment the conventional beamformer is not able to see the target as the beam is scanned through an angular region containing the target. Both the degraded and the fully operating antenna are blinded. Exceptions are lucky glimpses for the non-degraded antenna when pointing exactly two degrees off the target, due to deep and narrow nulls in beampattern SLL coinsiding with the jammer location for these pointing directions. However, the adaptive MVDR beamformer neutralizes the jammer and is also able to compensate for the defunct elements. Both the fully operating ULA as well as the 3-degraded ULA are able to see the target almost as good as if no jammer was present.

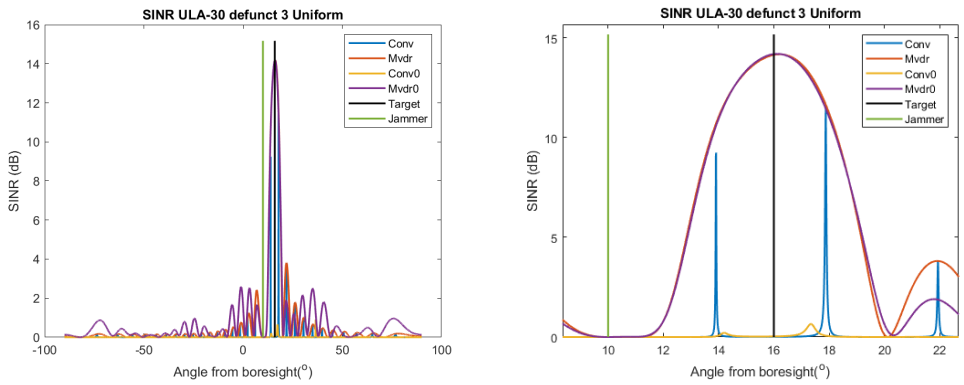

Figure 4.1 SINR beamscan for ULA-30 non-degraded and ULA-30 with three defunct elements [5,6,25]. Conv-BF non-degraded (blue), Conv-BF 3-degraded (yellow), MVDR-BF non-degraded (red), MVDR-BF 3-degraded (purple). Right panel zooms in on mainlobe.

Beamscan for the same signal environment using Dolph-Chebyshev tapering SLL -40dB is shown in Figur 4.2. The SLL for this tapered conventional beamformer is not low enough to suppress the jammer, and the target cannot be detected by the conventional beamformer. The MVDR beamformer with Dolph-Chebyshev tapering, however, sees the target well, both the fully operating and the 3-degraded antennas. The peak SINR obtained for the 3-degraded antenna is about 1dB less than the non-degraded antenna for this beamformer.

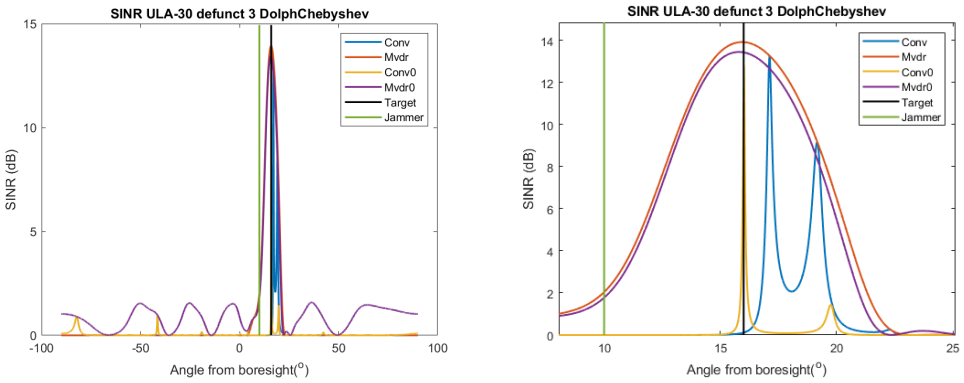

Figure 4.2 SINR beamscan for ULA-30 non-degraded and ULA-30 with three defunct elements [1,12,18]. Conv-BF non-degraded (blue) ,Conv-BF 3-degraded (yellow), MVDR-BF non-degraded (red), MVDR-BF 3-degraded (purple). All beamformers applied with Dolph-Chebyshev tapering. Right panel zoom on mainlobe.

The SINR array gain depends on how many elements L are defunct, and moreover which subset of L elements in the antenna of N elements are defunct. Figure 4.3 shows the distribution of SINR from conventional beamforming over the 3-degradations of the ULA-30 when pointing the beam exactly at the target location. The location and power received from jammer and target signal is identical to the one applied for Figure 4.1.

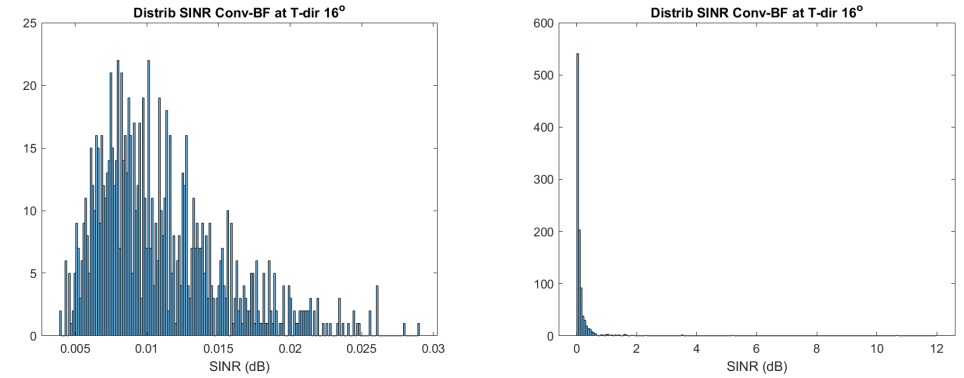

Figure 4.3 SINR Distribution of ULA-30 3-degradations after beamforming with Conventional without tapering (left panel) and with Dolph-Chebyshev tapering (right panel). 1000 random samples of 3-degradations are chosen. Input element-wise SNRe = 0*dB, and* JNRe = 40*dB.*

Both the conventional beamformer with Dolph-Chebyshev tapering and the one without tapering obtain a poor SINR for all the 3-degradations when exposed to the barrage jamming. Note that the abscissa in the left panel of Figure 4.3 spans a short interval close to zero dB. They are all blinded, like was shown for the fully operating antenna in Figures 4.1 and 4.2 when applied with the conventional beamformers.

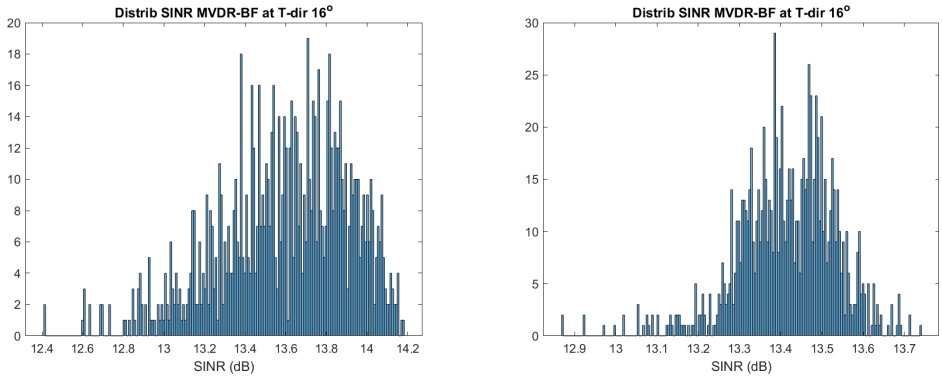

Figure 4.4 SINR Distribution of ULA-30 3-degradations after beamforming with MVDR without tapering (left panel) and with Dolph-Chebyshev tapering (right panel). 1000 random samples of 3-degradations are chosen.

The MVDR beamformer SINR response in the target direction for the 10% degradations of the array is nicely distributed close to the value obtained by the non-degraded array, as shown in Figure 4.4 and barely below the SINR to be expected for the uniform beamformer when there is no jamming, $10log10(N \cdot \text{SNRe}) = 14.77dB$.

To get information on what SINR gain can be expected when a given percentage of elements are defunct, we have calculated the mean value for the SINR of ULA-30 with three defunct elements when pointing the beam at the target, and where the mean is taken over 1000 random realisations among all 3-degradations. We have varied the target direction in a range of ±20° from the jammer located at 10° from boresight, and also varied the target signal strength so that the elementwise SNRe varies between 0 and 5 dB. For each combination the mean SINR is calculated when the antenna main beam is steered directly at the target. Results for the conventional-BF and the MVDR-BF both with Dolph-Chebyshev tapering are shown in Figure 4.5. The SINR value shown at a typical pixel in these figures is obtained by taking the mean over a histogram like Figure 4.3. To be specific, the SINR value in Figure 4.5 left panel at parameters SNRe=0dB and Angle from boresight=16° is obtained by taking the mean of the SINR distribution in Figure 4.3 right panel. And the SINR value at the same parameter location in the right panel of Figure 4.5 is obtained by taking the mean of the SINR distribution shown in the right panel of Figure 4.4. Right panel indicates the SINR is low when target location is close to the jammer location at 10° from boresight, for all the input target signal strengths shown. Located further than the main lobe beam width from the jammer, the SINR obtained by the MVDR is good, and increases smoothly with incrasing input target signal strength. The left panel indicates the SINR is always low for the conventional beamformer with Dolph-Chebyshev tapering for a barrage jammer of strength JNRe = $40dB$.

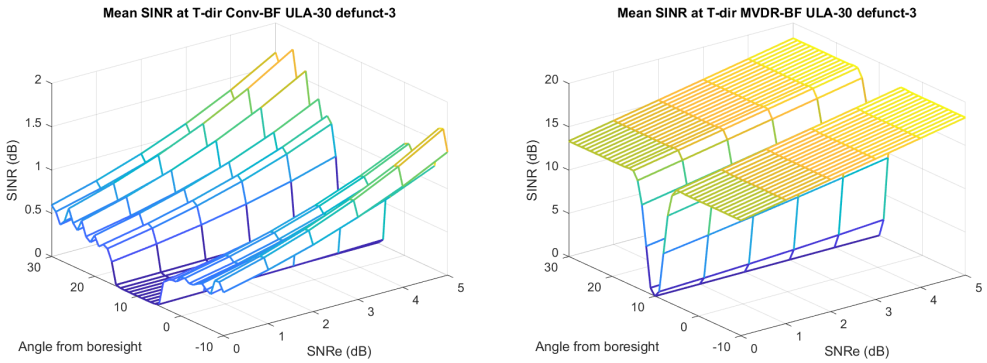

Figure 4.5 Mean SINR at target direction after beamforming for 1000 realisations of ULA-30 with three defunct elements, Conv-BF left panel and MVDR-BF right panel, both with Dolph-Chebyshev tapering. Input element-wise SNR and Target direction is varied, jammer at 10°.

For comparison purposes we show in Figure 4.6 the SINR achieved for the fully operating ULA-30 antenna by the Conventional-BF and MVDR-BF both with Dolph-Chebyshev tapering. The mean values obtained by the MVDR-BF for the 3-degradations shown in 4.5 are only about 1dB less than the values for the non-degraded antenna. The conventional beamformers behave badly in both cases.

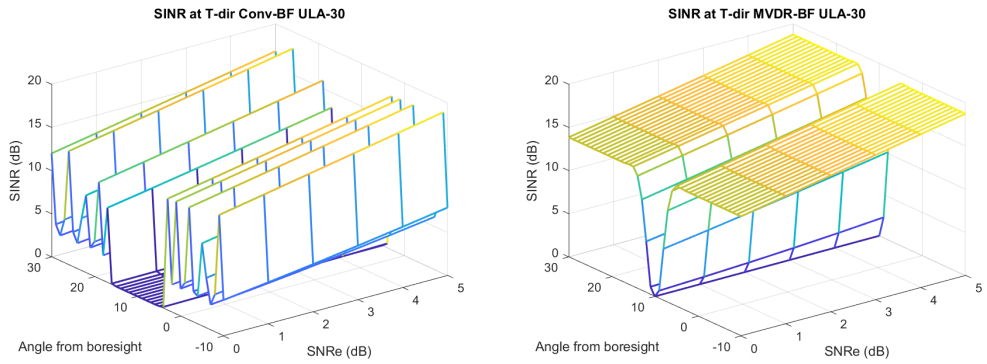

Figure 4.6 SINR at target direction after beamforming for the fully operating ULA-30 antenna, Conv-BF left panel and MVDR-BF right panel, both with Dolph-Chebyshev tapering.

As can be seen from Figures 4.1, and 4.2 showing the SINR as function of beam pointing direction, the SINR is not always the highest when the beam is steered directly towards the target. Sometimes higher array gain is achieved for pointing directions slightly to the side of the target. The distribution among the 3-degradations for the max SINR within the null-null beamwidth is shown in Figure 4.7. The target and jammer locations and signal strengths are the same as in Figure 4.3 above. We see that the spread for conventional BF is a bit wider in this case, but in general very low.

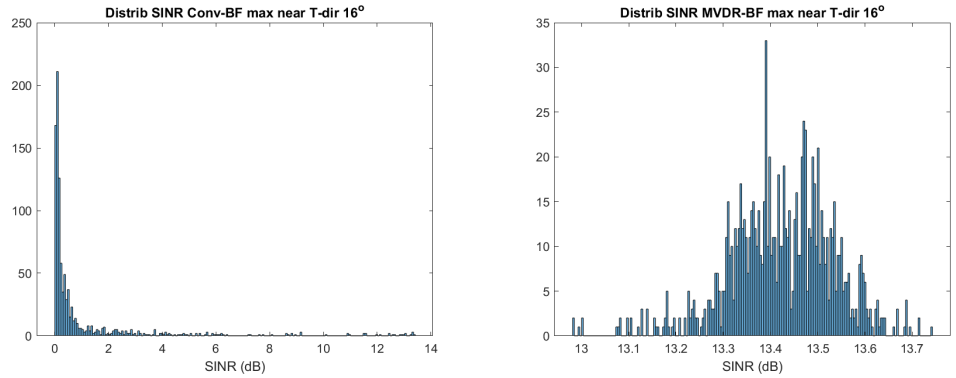

Figure 4.7 Distribution max SINR within null-null-Beam-width of target direction after beamforming for 1000 choices of ULA-30 with three defunct elements, Conv-BF left panel and MVDR-BF right panel, both with Dolph-Chebyshev tapering. Target at 16° *and Jammer at* 10° *from boresight,* SNRe = 0*dB,* JNRe = 40*dB.*

Figure 4.8 shows the mean value over 3-degradations for the maximum SINR within the main lobe null-null beam width from the target direction. Element wise input SNR is varied between 0 and 5 dB, and target direction of arrival is varied between $\pm 20^o$ from jammer location. Location of the jammer is fixed at 10°.

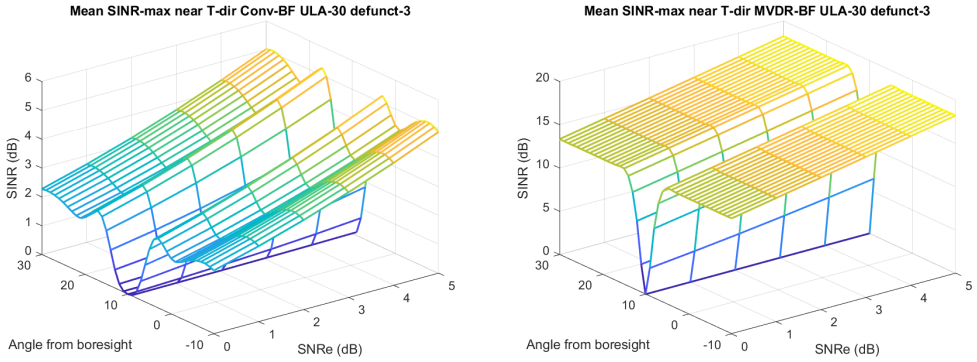

Figure 4.8 Mean for max SINR within null-null-Beam-width of target direction after beamforming for 1000 choices of ULA-30 with three defunct elements, Conv-BF (left panel) and MVDR-BF (right panel), both with Dolph-Chebyshev tapering. Input element-wise SNR and target direction from boresight is varied, jammer at 10°.

Comparing left panels of Figures 4.8 and 4.5 we see that the max SINR value within the main lobe null-null beamwidth for the conventional beamformer is still low, but nevertheless somewhat higher in general than the SINR value obtained by reading off exactly at the beam pointing direction towards the target. This holds when the target and jammer directions are not aligned, and is due to a lucky location of a beampattern side lobe null in the jammer direction. In a scenario with two or more jammers we would probably not see this difference, since the chance of luckily locating two or more nulls in the conventional beampattern directly at the locations of two or more jammers is very small. The right panels of the two figures show no difference, indicating that the max SINR values

obtained for the adaptive MVDR beamformer with three defunct elements are indeed located at the beam pointing direction towards the target. The MVDR beamformer manages to suppress the jammer even though three TRMs are defunct, and their locations in the array antenna do not seem to matter.

4.2 Diagonal loading

Diagonal loading is a common technique for making MVDR beamformer response more robust to fluctations in the input from array snapshots. Diagonal loading can be seen as adding white noise to the noise plus interference spatial covariance matrix when calculating the MVDR beamformer weights. In the extreme case, when the ratio between the maximum eigenvalues of the noise plus interference matrix and diagonal loading factor goes to zero, the diagonal loaded MVDR beamformer approaches the conventional beamformer. Let us briefly recapture this fact. The MVDR beamformer w_{mv} was given in (4.1) and the conventional beamformer in (4.3) The diagonally loaded MVDR beamformer is obtained by adding a positive weight σ to the covariance matrix diagonal,

$$w_{mvld} = K_\sigma^{-1} g / g^h K_\sigma^{-1} g \quad \text{where} \quad K_\sigma = K + \sigma I$$

The covariance matrix K is hermitian and has an orthonormal eigenvalue decomposition

$$K = V \Lambda V^h \quad \text{where} \quad V^h V = I \quad \text{and} \quad \Lambda = \text{diag}(\lambda_1, \ldots, \lambda_N)\,, \quad \lambda_j > 0$$

The diagonal elements λ_j of Λ are positive, and assuming some thermal noise they are all strictly positive. The diagonally loaded covariance matrix has a similar eigen-decomposition $K_\sigma = V \Lambda_\sigma V^h$ where Λ_σ is diagonal with diagonal elements $\lambda_j + \sigma$ all j. The inverse is $K_\sigma^{-1} = V \Lambda_\sigma^{-1} V^h$ where Λ_σ^{-1} is diagonal with diagonal elements $1/(\lambda_j + \sigma)$ all j. We note that $\sigma/(\lambda_j + \sigma) \to 1$ as $\lambda_j/\sigma \to 0$ and thus $\sigma K_\sigma^{-1} \to I$. We therefore have

$$w_{mvld} = \frac{K_\sigma^{-1} g}{g^h K_\sigma^{-1} g} \to \frac{g}{|g|_2^2} \quad \text{as} \quad \frac{\lambda_j}{\sigma} \to 0 \quad \text{all } j \tag{4.5}$$

Figure 4.9 shows the mean SINR in target direction among 1000 random 3-degradations of ULA-30 obtained by MVDR-BF with Dolph-Chebyshev tapering. The mean SINR is shown as function of diagonal loading factor for the MVDR beamformer and for various target directions to both sides of the jammer azimuth direction. The figure is shown with log10 scale (or 0.1dB scale) of the diagonal loading factor DL, where the diagonal loading added to the original covariance matrix is $\sigma = DL \cdot trace(K)/N$. Input signal strengths yields element-wise SNRe = $0dB$ and JNRe = $40dB$.

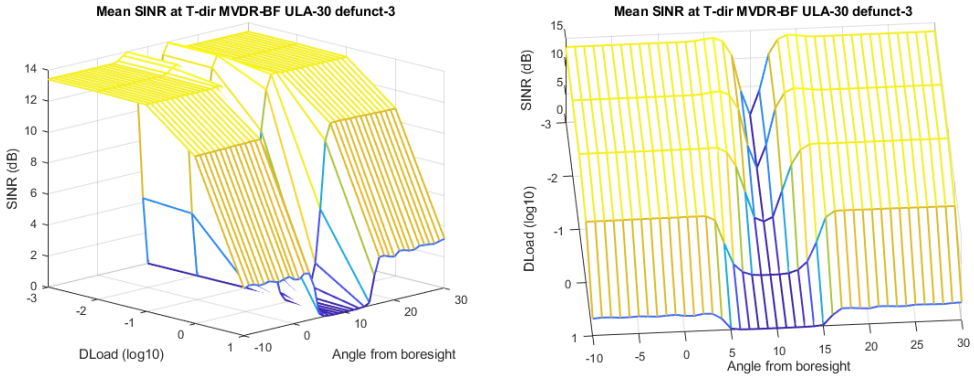

Figure 4.9 *Mean SINR at target direction after beamforming for 1000 choices of ULA-30 with three defunct elements, diagonally loaded MVDR BF. Target direction from Jammer is varied as well as Diagonal loading factor. Right panel is a rotation of the left panel.*

When the diagonal loading increases, the beamformer approaches the conventional beamformer with Dolph-Chebyshev tapering according to (4.5). In Figure 4.9 we can see the SINR achieved drops when the diagonal loading is substantial, also the angular separation between jammer and target must be well off the main lobe beam width for a reasonable SINR. The similar simulation is carried out for the full non-degraded ULA-30 antenna and depicted in 4.10

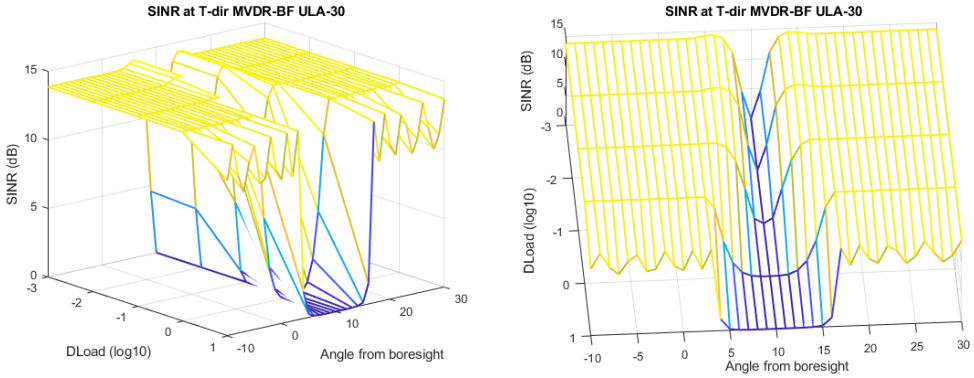

Figure 4.10 *SINR at target direction achieved by MVDR-BF with diagonal loading for a non-degraded ULA-30 antenna. Target direction from Jammer is varied as well as Diagonal loading factor. Right panel is a rotation of the left panel.*

The difference between Figure 4.10 and 4.9 is not significant for moderate diagonal loading values. Again indicating that the MVDR beamformer manages to compensate well for degradations. However, there is some difference between the figures when the diagonal loading increases. We observed in equation (4.5) that the MVDR beamformer approaches the conventional beamformer whith increasing diagonal loading. Figure 4.9 is an average over many realisations of 3-degradations, and near the end of the DLoad axis these are all almost conventional beamformers. Figure 4.10 shows the SINR obtained for a single beamformer over a full ULA-30, and this is an almost conventional beamformer at the end of the DLoad axis. In the latter case a lucky side lobe null will

enter the location of the jammer when the target and then beam direction is separated certain angles from the jammer. In Figure 4.9 showing the mean SINR over many 3-degradations the effect of such nulls is averaged out.

4.3 Array degradation and fully overlapping subarrays

A surveillance radar with a large rectangular array antenna may have more than thousand elements, and a TRM with full digitalization for each and every element is challenging for the signal processor. Grouping the antenna elements into subarrays with digitization of the signal output from each subarray is a remedy to this problem. The number of receiver channels producing data for the digital signal processor is thereby reduced to a managable size.

We have run simulations for a ULA antenna with fully overlapping subarrays and where some of the antenna elements are defunct. Fully overlapping subarrays in AESA antennas can be hardware implementations, but in our Matlab simulation code they are digital linear matrix filters, and the beamforming methods are referred to as beamspace methods. We assume there are M subarrays where each take input from all the N array elements of the antenna. Each subarray has one output channel and is a linear filter that can be updated every Coherent processing interval (CPI), but is fixed during the CPI and does not depend on the incoming signals. The subarray filters are implemented as a complex matrix T of size $N \times M$, and we assume the matrix T has full rank M with $M \leq N$. When x is a snapshot from the full array antenna, the subarray output is $\tilde{x} = T^h x$. To discriminate between the output directly from the antenna element array and the output after filtering with the matrix T, we will use the phrase 'element-space' to describe the first and 'beam-space' about the latter. A Beamspace (BS) beamformer $\tilde{w}$ is a linear filter made by a complex M vector, and the beamspace beamformer response is

$$\tilde{w}^h \tilde{x} = \tilde{w}^h T^h x$$

The beamspace noise plus interference spatial covariance matrix is $\tilde{K} = \varepsilon\left(T^h x x^h T\right) = T^h K T$ and the correlation matrix is $\tilde{R} = T^h R T$ where K and R are the element space covariance- and correlation matrices. Finally we have adopted the beamspace SINR as

$$\text{SINR} = \frac{\tilde{w}^h \tilde{R} \tilde{w}}{\tilde{w}^h \tilde{K} \tilde{w}} \ .$$

Two beamformers are considered. The first is the beamspace MVDR beamformer $\tilde{w}_{mv}$ solving

$$\min \tilde{w}^h \tilde{K} \tilde{w} \ \text{ subject to } \tilde{w}^h \tilde{g} = 1$$

where the desired beamspace response vector is $\tilde{g} = T^h g$, and g is the element space desired response vector. Typically $g = t \odot s$ where t is the element array tapering vector, and $s = s(\eta)$ is the element space steering vector in the desired direction η. Like the element space MVDR beamformer (4.1) solves a quadratic problem, the solution to the current similar beamspace quadratic problem is

$$\tilde{w}_{mv} = \alpha \tilde{K}^{-1} \tilde{g} = \alpha \left(T^h K T\right)^{-1} T^h g \ \text{ where } \alpha^{-1} = \tilde{g}^h \tilde{K}^{-1} \tilde{g} = g^h T (T^h K T)^{-1} T g \qquad (4.6)$$

The other beamformer considered is the beamspace conventional beamformer. This is obtained by replacing the element space covariance matrix K in (4.6) by the identity matrix, that is assuming

thermal noise only and no other interference

$$\tilde{w}_c = \frac{(T^hT)^{-1}\tilde{g}}{\tilde{g}^h(T^hT)^{-1}\tilde{g}} = \frac{(T^hT)^{-1}T^hg}{g^hT(T^hT)^{-1}T^hg} \tag{4.7}$$

We have assumed T to have full rank M, but a common and more restrictive requirement for the beamspace matrix is that the columns are orthonormal, $T^hT = I$, [4]. In this case we retrieve the familiar form $\tilde{w}_c = \tilde{g}/|\tilde{g}|^2$ for the conventional beamformer.

For an ULA-N antenna with defunct elements it is convenient to consider the submatrix T_0 of T consisting of the elements in T corresponding to the fully operational elements only. Like in the paragraph leading up to equation (4.4) we let J_0 be the set of $N - L$ indices corresponding to the fully operating antenna elements of the given L-degradation. The subarray of a snapshot x from the array output corresponding to the operational elements is $x_0 = x(J_0)$, and the elements of T_0 are

$$T_0(i, j) = T(J_0(i), j)$$

The effect of the filter matrix T on the snapshot x can then be written $T^hx = T_0^hx_0$. We note that a possible orthonormal columns property of T might be lost in T_0. For an L-degradation the beamspace covariance matrix takes the form

$$\tilde{K} = \varepsilon(T^hxx^hT) = T_0^hK_0T_0$$

where K_0 is the element-space covariance matrix for the L-degradation. Similarly the beamspace correllation matrix may be written in terms of the element-space L-degraded correllation matrix, $\tilde{R} = T_0^hR_0T_0$. The L-degradation beamspace MVDR beamformer $\tilde{w}_{0mv}$ and conventional beamformer $\tilde{w}_{0c}$ are defined by replacing T, K, g in (4.6) and (4.7) by T_0, K_0, g_0.

In our simulations we define T for the ULA-30 antenna as follows. Let θ_D be the desired beam pointing direction with u-space coordinate $u_D = \sin\theta_D$. Let $u_m = u_D + \frac{m}{N}\frac{\lambda}{d}$ for $m \in \{0, 1, \ldots, M-1\} - (M-1)/2$. The columns of T are taken as the steering vectors in directions $\theta_m = \text{asin}(u_m)$, that is

$$T_{jm} = \exp\left(i\frac{2\pi}{\lambda}dju_m\right)/\sqrt{N} = \exp\left(i2\pi\left(\frac{d}{\lambda}ju_D + \frac{jm}{N}\right)\right)/\sqrt{N}$$

for $j = (1-N)/2, \ldots, (N-1)/2$, $m = (1-M)/2, \ldots, (M-1)/2$. We note that this T obeys the orthonormal columns requirement. When applied to a steering vector in direction u the filter output from the matrix T applied to u will trace out M sinc curves as u travels through u-space, alternatively as $\theta = \text{asin}(u)$ traces out the half circle with circle segment midpoint at the antenna boresight. Figure 4.11 depicts the fan of response beams from the T filter as the steering vector argument runs through the angle interval $(-90, 90)^\circ$ from boresight. Dolph-Chebyshev tapering is applied. The right panel shows the fan of response beams for the ULA-30 with the three defunct elements number [1,12,18]. We note that this set of three defunct elements very much destroys the low SLL for the Dolph-Chebyshev tapering, from -40dB for the non-degenerate array in the left panel to -20dB in the right panel for this 3-degradation.

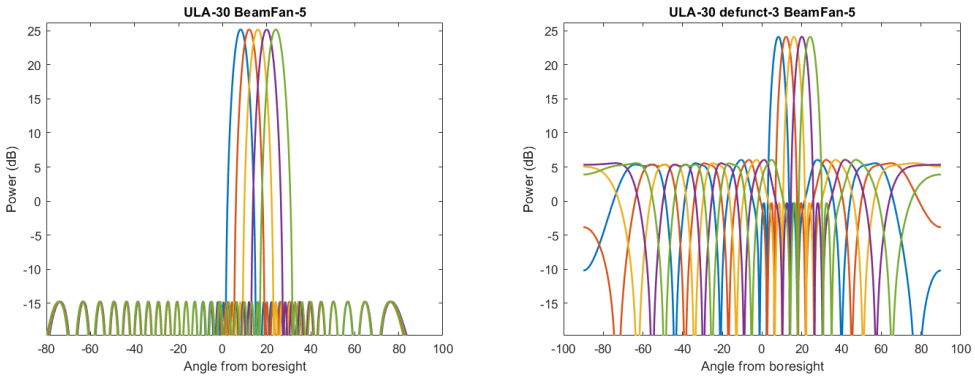

Figure 4.11 *Response beams for ULA-30 from Beamspace filter of five beams traced out as the steering vector with Dolph-Chebyshev tapering runs through all directions in the half circle with midpoint at boresight. Beam fan is centered at* 20°. *Left panel depicts non-degraded array, Right panel depicts array with the three defunct elements.*

Our simulations testing the impact of defunct elements on the SINR achieved by beamspace methods have all been run for a ULA-30 anteanna with five fully overlapping subarrays. The subarray response beams make a fan centered at the array pointing direction. The antenna has 10% degradation, that is three elements are defunct. The BS beamformers BS-Conventional and BS-MVDR with and without Dolph-Chebyshev tapering are testet. Diagonal loading with factor 0.1 relative to the normalized trace of the covariance matrix is applied for the BS-MVDR beamformer.

In the first example there is a jammer located at 10° and target at 16° with signal strengths resulting in elementwise JNRe $= 40dB$ and SNRe $= 0dB$. The array elements $[1, 12, 18]$ are defunct. Figure 4.12 shows the beamspace SINR achieved from beamscan by the BS-Conventional- and the BS-MVDR beamformer, both with Dolph-Chebyshev tapering. The beam is scanned throught ±90° from boresight in order to obtain insight in the BS beamformer behavior. In practice the beam would not be scanned outside the **fan sector** defined as *the angular interval from the first left null in the first beam to the first right null in the last beam of the fan*. Also the SINR attained for a fully non-degraded ULA-30 with five subarrays and the same beamformers are depicted. Right panel zooms in on the main lobe angular area. Like for the element-space method in Section 4.1, the MVDR method gives high SINR when steering at the target, whereas the conventional behaves badly. When scanning the beam outside the fan sector the SINR response do not behave well.

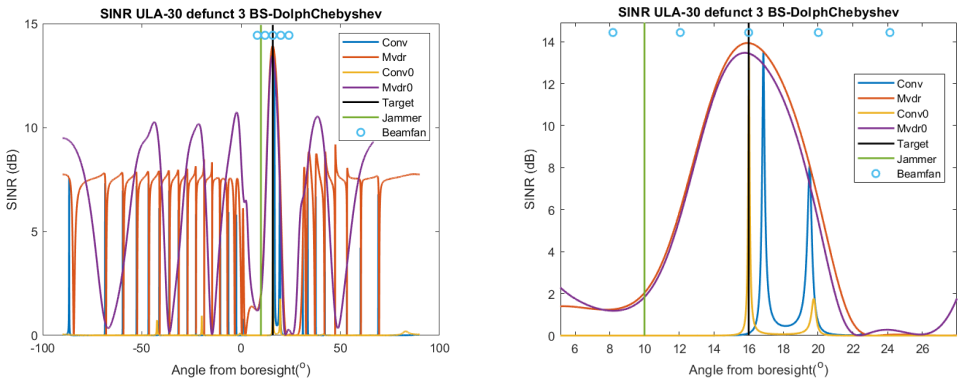

Figure 4.12 SINR beamscan for ULA-30 BS-5 non-degraded and ULA-30 BS-5 with three defunct elements [1,12,18]. The beamformers are BS-Conv-BF non-degraded (blue), BS-Conv-BF 3-degraded (yellow), BS-MVDR-BF non-degraded (red), BS-MVDR-BF 3-degraded (purple). Beam fan has five beams and all beamformers applied with Dolph-Chebyshev tapering. Right panel zooms in on main lobe.

Figure 4.13 shows the SINR distribution over all 3-degradations obtained by the BS-Conv and BS-MVDR beamformers for the ULA-30 with fan of five beams where the beam-fan is centered at the target direction. Also, the beamformed main lobe is pointing in the same direction as the fan center, i.e at the target.

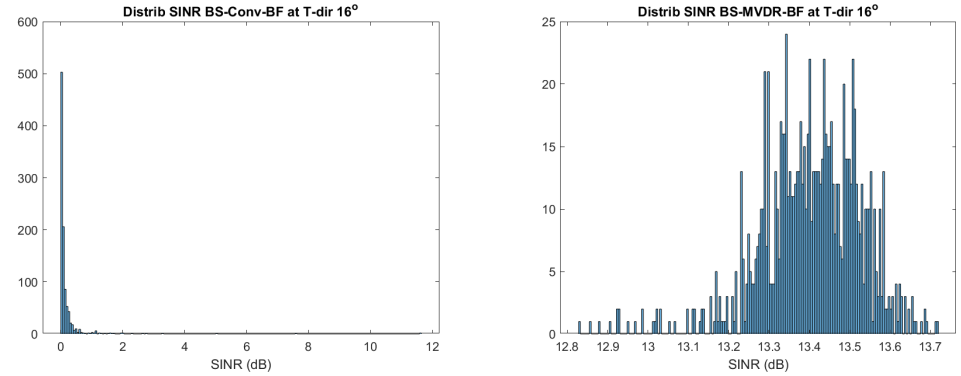

Figure 4.13 SINR Distribution after beamforming for 3-degradations of ULA-30 with five beams. Left panel shows BS-Conv-BF and right panel BS-MVDR-BF, both with Dolph-Chebyshev tapering. 1000 random samples of 3-degradations are chosen.

The average SINR in target direction after beamspace beamforming for 1000 random 3-degradations of ULA-30 is shown in Figure 4.14. There are five beams in the beam-fan and the fan is centered at the target direction and the main lobe is steered to the fan center. The mean is shown as a function of target signal DoA and strength. The DoA varies within the interval $(-10, 30)°$ from boresight and element-wise SNRe is within $0dB$ to $5dB$. The jammer has fixed location at 10° from boresight and element-wise interference to noise ratio is JNRe = $40dB$. The left panel depicts results for the BS-Conv-BF and the right for the BS-MVDR-BF, both with Dolph-Chebyshev tapering. The left

behaves badly, in particular for the jammer located closer to the target than half the fan-sector width. The BS-MVDR beamformer manages to suppress the jammer as long as the jammer is located well within the fan-sector but not too close to the main lobe center axis. These properties are even more apparent for the non-degraded antenna in Figure 4.15.

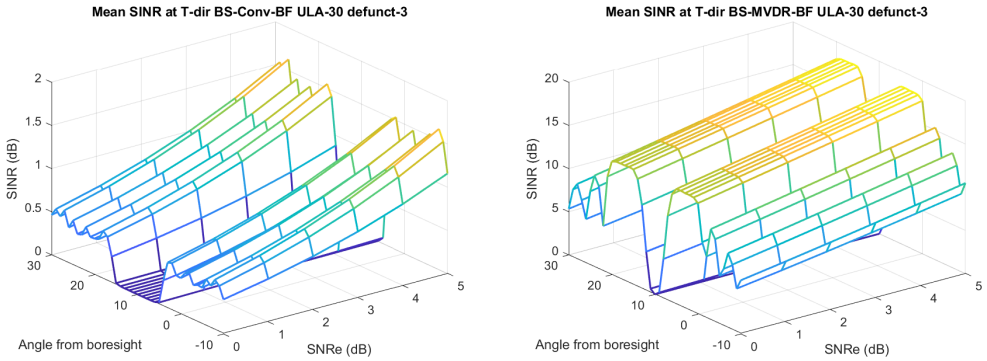

Figure 4.14 Mean SINR at target direction after beamforming for 1000 choices of ULA-30 with three defunct elements, BS-Conv (left panel) and BS-MVDR (right panel), both with Dolph-Chebyshev tapering, and fan of five beams. Input element-wise SNR and Target direction from Jammer is varied.

The mean values obtained by the MVDR beamformer for the 3-degradations in Figure 4.14 are less than 1dB below the values for the non-degraded antenna in Figure 4.15 as long as the jammer is located well inside the fan sector. The conventional beamformers behave badly in both cases.

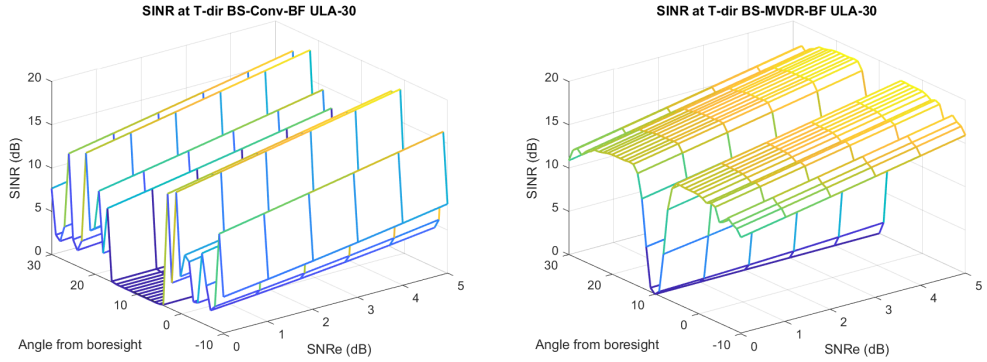

Figure 4.15 SINR at target direction after beamforming for the fully operating ULA-30 antennna, BS-Conv in left panel and BS-MVDR in right panel, both with Dolph-Chebyshev tapering. Fan beam has five beams.

The simulations indicate the BS-MVDR with a fan of beams from a few fully overlapping subarrays mitigate well the interference from a barrage jammer as long as the jammer appears close to the main lobe, that is within the fan sector. In this case the response of the subarray beams to the interference signal is high enough to make a solid null in direction of the jammer while simultaneously giving a strong response to the target signal. This holds for the fully operating ULA-30 antenna as well as

for the 10% degraded antenna. When the jammer is further separated from the target the fan of beams is not able to achieve these two simultaneous goals. Other techniques like side lobe canceller might be more beneficial for suppressing the interferring signal in that case.

5 Concluding remarks

The conducted simulations indicate the ULA with a TRM for each antenna element tolerates well 10% degradation as long as the appropriate signal processing is adopted. The MVDR beamformer adapted to the current degradation mitigates well the interference from a barrage jammer. Simulations have also been run for an ULA-30 with a few fully overlapping subarrays with an analog-digital converter for each subarray. Also in this case the adapted MVDR mitigate well the barrage jammer as long as the jammer and target are separated less than the fan sector, although not when they are located along the same line from the antenna location. The conventional beamformers are blinded by the barrage jammer, both the fully operating ULA and the 10% degraded ULA.

In transmit mode the conventional beamformer was tested. Simulations show that the maximum directivitiy is not altered much by 10% degradation. For the conventional beamformer without tapering this was to be expected since in this case the max directivity is determined by the number of operating elements in the linear array. However, the degradation has a notable effect on the SLL, and in particular for conventional beamformers with non-uniform tapering. The Dolph-Chebyshev low SLL tapering for the full array is very much impaired by the defunct elements.

A Acronyms

ABF Adaptive Beamforming
AESA Active electronically scanned array
BF Beamforming
BS Beamspace
CPI Coherent processing interval
DBF Digital beamforming
DoA Direction of Arrival
DoF Degrees of Freedom
JNR Jamming to Noise Ratio
INR Interference to Noise Ratio
MVDR Minimum Variance Distortionless Response
PESA Passive electronically scanned array
SINR Signal to Interference plus Noise Ratio
SLL Side lobe level
SNR Signal to noise ratio
TRM Transmit Receive Module
ULA Uniform Linear Array

References

[1] D. Aalfs. Adaptive digital beamforming. In W. L. Melvin and J. A. Scheer, editors, *Principles of Modern Radar, volII Advanced Techniques*, chapter 9. SciTech Publishing, 2013.

[2] D.H. Johnson and D.E. Dudgeon. *Array Signal Processing*. Prentice-Hall Inc, 1993.

[3] W.L. Melvin. Clutter suppression using space-time adaptive processing. In W. L. Melvin and J. A. Scheer, editors, *Principles of Modern Radar, volII Advanced Techniques*, chapter 10. SciTech Publishing, 2013.

[4] H. Van Trees. *Detection, Estimation, and Modulation Theory, Optimum Array Processing, (Part IV)*. John Wiley & Sons,Inc., New-York, USA, ISBN 0-471-09390-4, 2002.

About FFI

The Norwegian Defence Research Establishment (FFI) was founded 11th of April 1946. It is organised as an administrative agency subordinate to the Ministry of Defence.

FFI's mission

FFI is the prime institution responsible for defence related research in Norway. Its principal mission is to carry out research and development to meet the requirements of the Armed Forces. FFI has the role of chief adviser to the political and military leadership. In particular, the institute shall focus on aspects of the development in science and technology that can influence our security policy or defence planning.

FFI's vision

FFI turns knowledge and ideas into an efficient defence.

FFI's characteristics

Creative, daring, broad-minded and responsible.

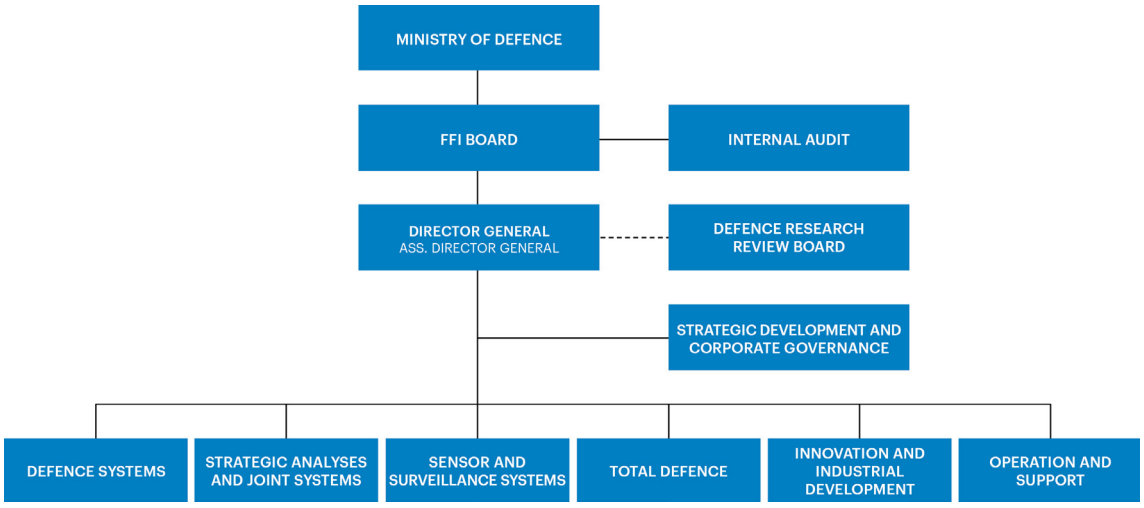

Forsvarets forskningsinstitutt
Postboks 25
2027 Kjeller

Besøksadresse:
Instituttveien 20
2007 Kjeller

Telefon: 63 80 70 00
Telefaks: 63 80 71 15
Epost: post@ffi.no

Norwegian Defence Research Establishment (FFI)
P.O. Box 25
NO-2027 Kjeller

Office address:
Instituttveien 20
N-2007 Kjeller

Telephone: +47 63 80 70 00
Telefax: +47 63 80 71 15
Email: post@ffi.no